ORIGINAL ARTICLE

DEPTOR is a direct NOTCH1 target that promotes cell proliferation and survival in T-cell leukemia

Y Hu[1,8], H Su[2,8], C Liu[1], Z Wang[1], L Huang[3], Q Wang[4], S Liu[5], S Chen[4], J Zhou[3], P Li[6], Z Chen[2], H Liu[7] and G Qing[7]

Aberrant activation of NOTCH1 signaling plays a vital role in the pathogenesis of T-cell acute lymphoblastic leukemia (T-ALL). Yet the molecular events downstream of NOTCH1 that drive T-cell leukemogenesis remain incompletely understood. Starting from genome-wide gene-expression profiling to seek important NOTCH1 transcriptional targets, we identified DEP-domain containing mTOR-interacting protein (DEPTOR), which was previously shown to be important in multiple myeloma but remains functionally unclear in other hematological malignancies. Mechanistically, we demonstrated NOTCH1 directly bound to and activated the human *DEPTOR* promoter in T-ALL cells. DEPTOR depletion abolished cellular proliferation, attenuated glycolytic metabolism and enhanced cell death, while ectopically expressed DEPTOR significantly promoted cell growth and glycolysis. We further showed that DEPTOR depletion inhibited while its overexpression enhanced AKT activation in T-ALL cells. Importantly, AKT inhibition completely abrogated DEPTOR-mediated cell growth advantages. Moreover, DEPTOR depletion in a human T-ALL xenograft model significantly delayed T-ALL onset and caused a substantial decrease of AKT activation in leukemic blasts. We thus reveal a novel mechanism involved in NOTCH1-driven leukemogenesis, identifying the transcriptional control of DEPTOR and its regulation of AKT as additional key elements of the leukemogenic program activated by NOTCH1.

Oncogene advance online publication, 5 September 2016; doi:10.1038/onc.2016.275

INTRODUCTION

Acute T-cell lymphoblastic leukemia (T-ALL) is an aggressive malignant disorder of T-cell progenitors, accounting for 10–15% of pediatric and 25% of adult acute lymphoblastic leukemia cases.[1] Despite major therapeutic improvements due to treatment intensification and refined risk-adapted stratification during the past decade, ~30% of T-ALL cases relapse with very poor prognosis.[2] Ongoing studies are still fueled to understand the precise molecular mechanisms underlying the disease development and recurrence. The identifications of NOTCH1-activating mutations[3] and FBW7 mutations[4,5] in T-ALL patients highlight the major role of aberrant NOTCH1 signaling in the pathogenesis of T-ALL.[6] Normally, NOTCH1 receptors are activated by binding of the delta-serrate-lag2 ligands, triggering a series of proteolytic cleavages and resulting in γ-secretase-generated intracellular NOTCH1 that activates responder gene expression in the nucleus.[7,8] Mutations identified in T-ALL potentiate the signal strength by either eliciting ligand-independent activation or prolonging ICN1 half-life. The precise mechanisms by which aberrant NOTCH1 signaling causes T-ALL probably entail aberrant expression of oncogenic responder genes such as *MYC*.[9,10] However, enforced MYC expression seems insufficient to restore γ-secretase inhibitor (GSI) -mediated growth arrest in a subset of T-ALL cell lines,[10] and NOTCH1 mutations potentiate the leukemogenic effects in murine MYC transgenic T-ALL,[11]

suggesting that NOTCH1 functions through concerted regulation of multiple downstream targets in addition to *MYC*. Despite enormous efforts made to determine other NOTCH1 targets essential for T-ALL,[10,12–19] their identities, functions and mechanisms of regulation are incompletely understood.

DEP-domain containing mTOR-interacting protein (DEPTOR) emerges as an endogenous mTOR inhibitor that binds to and represses mTORC (mTOR complex) 1 and 2,[20] implicated in vascular endothelial cell activation,[21] adipogenesis[22] and glucose homeostasis.[23] Being an inhibitory mTOR partner, DEPTOR expression is frequently low in most solid tumors[20] but paradoxically high in a subset of multiple myelomas,[20,24,25] where its overexpression leads to AKT activation through alleviating feedback inhibition from mTORC1 to PI3K signaling.[26,27] It appears that specific genetic contexts and tumor types determine the way DEPTOR engages in turmorigenesis, resulting in either oncogenic or tumor-suppressive phenotypes. The complexity of DEPTOR involvement in tumorigenesis raises important questions whether DEPTOR overexpression occurs in other type(s) of cancers and what mechanism(s) are employed to control the context-dependent DEPTOR activation.

One of the mechanisms that NOTCH1 promotes leukemogenesis is through cooperation with AKT,[28,29] which has a central role in cell survival, proliferation and chemotherapeutic resistance.[30,31] Palomero *et al.*[29] have linked NOTCH1 to AKT through

---

[1]School of Pharmacy, Tongji Medical College, Huazhong University of Science and Technology, Wuhan, People's Republic of China; [2]Institute of Hematology, Union Hospital, Tongji Medical College, Huazhong University of Science and Technology, Wuhan, People's Republic of China; [3]Department of Hematology, Tongji Hospital, Tongji Medical College, Huazhong University of Science and Technology, Wuhan, People's Republic of China; [4]Key Laboratory of Thrombosis and Hemostasis of Ministry of Health, Jiangsu Institute of Hematology, The First Affiliated Hospital of Soochow University, Suzhou, People's Republic of China; [5]Department of Pediatric Hematology, Tongji Hospital, Tongji Medical College, Huazhong University of Science and Technology, Wuhan, People's Republic of China; [6]Key Laboratory of Regenerative Biology, South China Institute for Stem Cell Biology and Regenerative Medicine, Guangzhou Institutes of Biomedicine and Health, Chinese Academy of Sciences, Guangzhou, People's Republic of China and [7]Medical Research Institute, Wuhan University, Wuhan, People's Republic of China. Correspondence: Professor H Liu or Professor G Qing, Medical Research Institute, Wuhan University, 185 Donghu Rd, Wuhan, Hubei 430071, P. R. China.
E-mail: hudanliu@whu.edu.cn or qingguoliang@whu.edu.cn
[8]These authors contribute equally to the work.

transcriptionally activating *HES1*, which represses PTEN, the negative regulator of PI3K/AKT. However, whether PTEN downregulation is exclusively responsible for aberrant AKT activation or other oncogenic programs are involved remains unclear. We herein present a novel mechanism that NOTCH1 alternatively activates AKT through direct transcriptional activation of *DEPTOR*. The essential roles of DEPTOR in T-ALL shed new light in understanding the pathophysiology of NOTCH1-mediated T-cell leukemogenesis.

RESULTS

Identification of *Deptor* as a NOTCH1 downstream target gene in murine T-ALL

To screen additional novel NOTCH1 downstream target genes, we performed gene-expression profiling in a murine T-ALL cell T6E. This cell line expresses a gain-of-function truncation of human NOTCH1 such that signaling activation is independent of ligand but requires γ-secretase-mediated cleavage to create ICN1.[32] T6E cells were treated with GSI *N*-[*N*-(3,5-Difluorophenacetyl-*L*-alanyl)]-*S*-phenylglycine *t*-butyl ester (DAPT) (1 μM) or dimethylsulfoxide (DMSO) for 12 h, then harvested for RNA preparation and subsequent array analysis. We identified a total of 70 genes whose expressions were most sensitive to DAPT treatment (Figure 1a and Supplementary Table S1). Downregulated genes included previously characterized NOTCH1 targets in T-cell progenitors or T-ALL (*Dtx1*, *Nrarp*, *Hes1* and *Myc*) (Figure 1a). *Deptor*, which ranks the top five among those significantly repressed by DAPT (Figure 1a), gained our attention given its implication in AKT signaling activation.[20,23] We then validated these findings in T6E using alternative approaches. Administration of Compound E, another specific GSI, consistently induced a dramatic downregulation of DEPTOR at both mRNA and protein levels (Figure 1b). The decreased DEPTOR expression was due to NOTCH1 inactivation as Compound E similarly blocked ICN1 processing and the expression of MYC, a well-characterized NOTCH1 target[10] (Supplementary Figure S1a). More specific NOTCH inhibition by dominant negative Mastermind-like 1 (MAML) expression via retroviral transductions also caused a noticeable decline in DEPTOR abundance (Figure 1c). Similar effect was observed in the expression of MYC (Supplementary Figure S1a). Importantly, reciprocal overexpression of ICN1 reconstituted NOTCH1 activity in the presence of Compound E and markedly reversed the GSI-induced DEPTOR and MYC downregulation (Figure 1d and Supplementary Figure S1a), demonstrating that NOTCH1 activity is sufficient and required for the DEPTOR expression in murine T-ALL cells.

DEPTOR is regulated by NOTCH1 signaling in human T-ALL

We further evaluated the DEPTOR expression in human T-ALL cells to ensure the NOTCH1 regulation of DEPTOR across species. In five human T-ALL cell lines, administration of Compound E blocked ICN1 processing (Supplementary Figure S1b), concomitant with marked inhibition of *DEPTOR* expression (Figure 2a). NOTCH inhibition by dominant negative MAML expression also decreased the *DEPTOR* mRNA in HPB-ALL cells (Figure 2b). Notably, decline in *DEPTOR* mRNA levels corresponded to respective protein abundance (Figure 2c). We next systematically analyzed the *DEPTOR* expression in 506 B-ALL and 174 T-ALL primary samples as provided by Haferlach *et al*.[33] Compared with normal peripheral blood, *DEPTOR* expression was profoundly elevated in a subset of T-ALL exhibiting higher NOTCH1 activity, as reflected by the increased expression of *NOTCH1* or *HES1* (Figure 2d and Supplementary Figure S2). In contrast, *DEPTOR* mRNA levels were significantly lower in B-ALL (Figure 2d), similar to many other tumors.[20] We further verified these findings in 18 cDNA samples obtained from domestic Chinese T-ALL patients and observed a significant correlation between *DEPTOR* and *HES1* expression

(*R* = 0.9830, *P* < 0.001; Figure 2e). Due to lack of associated protein extracts with the cDNA specimens, we retrieved an additional 7 primary T-ALL protein extracts and found that DEPTOR was generally more abundant in leukemia cells exhibiting stronger NOTCH1 activation, as judged by ICN1 production (Figure 2f). Thus, in addition to multiple myelomas,[20] *DEPTOR* is highly expressed in a subset of T-ALL samples exhibiting aberrant NOTCH1 activation.

NOTCH1 directly activates *DEPTOR* transcription

To examine whether NOTCH1 directly activates *DEPTOR* transcription, we performed a GSI-washout experiment, which had been successfully applied in the identification of NOTCH1 targets *MYC*[10] and *HRB*,[34] in T6E and SIL-ALL cells. Notably, Compound E washout immediately reversed the inhibitory effects of Compound E on *DEPTOR* expression within 2 h, and these effects were even more pronounced at the 4 h time point (Figure 3a). In contrast, minimal changes were observed in mock-treated cells. Such a swift rebound of *DEPTOR* mRNA suggests that NOTCH1 activation of *DEPTOR* expression occurs directly at the transcriptional level. In support of this notion, we identified two conserved CSL-binding consensus sequences among a variety of species, which are proximal to the transcription initiation site (Figure 3b). We created a luciferase reporter construct containing the putative CSL-binding site to directly test whether loading of NOTCH1 is required for *DEPTOR* activation. As expected, ICN1 strongly activated the reporter gene containing wild-type CSL-binding site while exhibited minimal effect on the mutant one (Figure 3c). The *HES1* reporter gene containing a well-characterized CSL site was used as a positive control. We next performed chromatin immunoprecipitation and revealed that, compared with the control IgGs, antibodies against NOTCH1 specifically pulled down the *DEPTOR* and *HES1* promoter DNAs, but not the *ACTIN* promoter DNA (Figure 3d). These observed associations were rapidly diminished in the presence of Compound E (Figure 3d). Previous ChIP-Seq data revealed a potential NOTCH1-binding site, ~ 1.25 Mb upstream of the *DEPTOR* gene, which may contribute to NOTCH1-mediated *DEPTOR* transcription.[18,19,35] However, inclusion of this distal site upstream of the *DEPTOR* promoter failed to induce a synergistic or additive effect on luciferase activity (Supplementary Figure S3), implying irrelevance of this element for *DEPTOR* expression. Our data thus provide strong evidence that NOTCH1 transcriptional complexes directly bind to the *DEPTOR* promoter and activate its transcription.

DEPTOR has a vital role in T-ALL cell proliferation, viability and metabolism

We next sought to determine potential roles of DEPTOR in T-ALL by short-hairpin RNA (shRNA) -mediated DEPTOR ablation in HPB-ALL and MOLT4 cells. The shRNA was cloned into a modified pLKO.1 vector, in which the puromycin resistant gene was replaced by the *GFP* gene.[36] GFP^{+} cells, representing shRNA-expressing populations, were analyzed for growth rates. As shown in Figure 4a, DEPTOR-depleted GFP[+] HPB-ALL and MOLT4 cells exhibited growth inhibition in comparison with those expressing a control shRNA. Whereas percentages of GFP^{+} cells infected with control shRNA remained minimally changed, GFP[+] percentages dramatically declined over time in those transduced with a DEPTOR shRNA (Figure 4b). Similar results were obtained with another shRNA specifically targeting *DEPTOR* (Supplementary Figure S4a). It seemed that DEPTOR depletion induced marked apoptosis in HPB-ALL and MOLT4 cells (Figure 4c and Supplementary Figure S4b), but barely affected cell cycle (Supplementary Figure S4c). In addition, DEPTOR inactivation inhibited glucose uptake concomitant with substantial decrease in lactate secretion (Figure 4d). Conceivably, the enhanced apoptosis and decreased glycolysis may contribute to the observed growth inhibition.
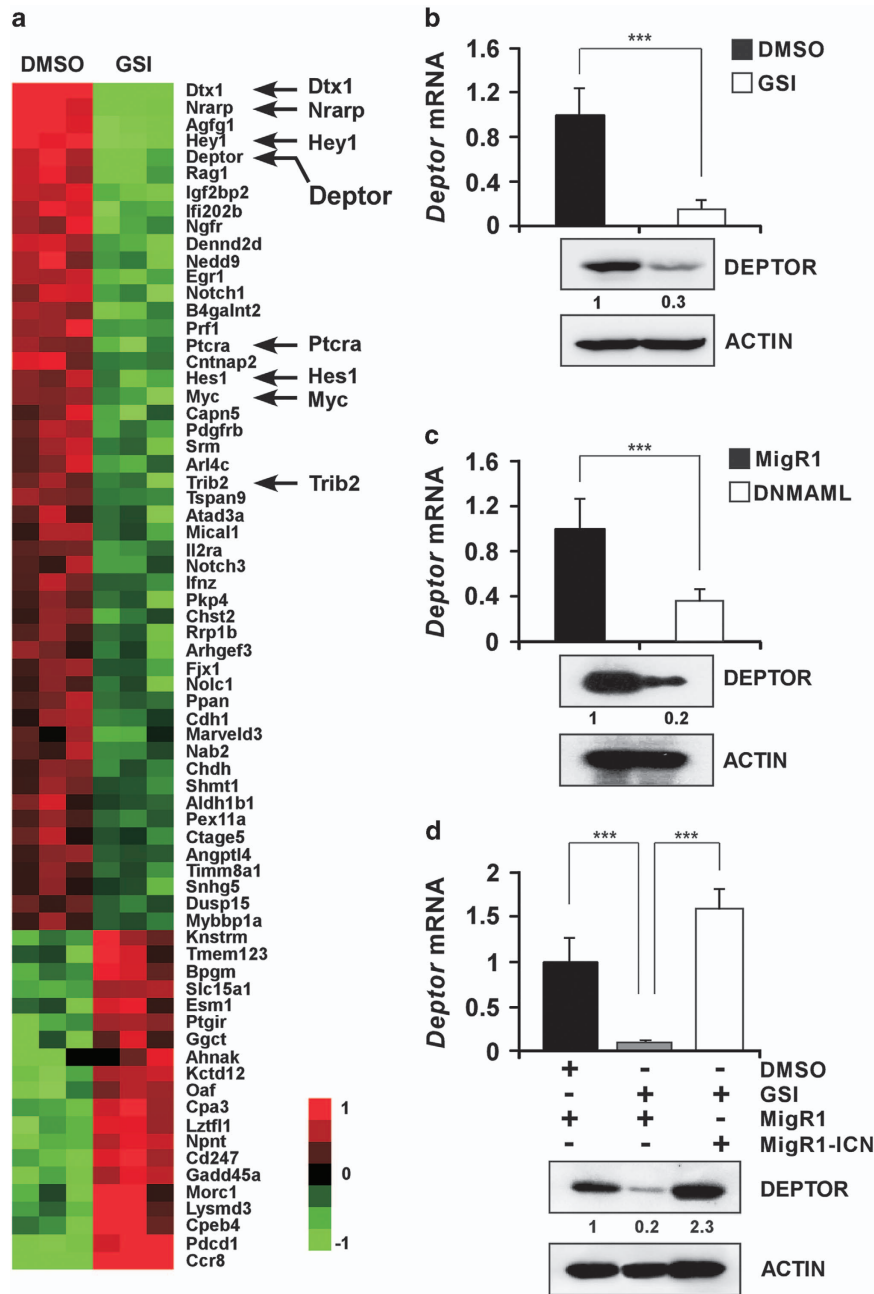
Figure 1. *Deptor* is a NOTCH1 downstream target gene in murine T-ALL. (**a**) Heatmap representation of differentially expressed genes upon NOTCH inhibition. The top 70 genes whose expressions were significantly changed upon NOTCH inactivation ($P < 0.05$) are shown. The scale bar shows color-coded differential expression. Red: increased expression; and green: decreased expression. (**b, c**) NOTCH inhibition downregulated DEPTOR in murine T-ALL. *Deptor* mRNA and protein levels were quantified in T6E cells by real-time qPCR and immunoblotting upon Compound E (1 μM) or DMSO treatment for 48 h in **b** or upon infection with indicated retroviruses in **c**. (**d**) Enforced ICN1 expression reversed GSI-mediated DEPTOR downregulation. T6E cells were transduced with indicated retroviruses and treated with Compound E (1 μM) for 48 h before DEPTOR mRNA and protein quantifications. Data were presented as the mean values (± s.d.) of triplicate wells. ***$P < 0.001$. qPCR, quantitative PCR.

Conversely, enforced expression of DEPTOR by lentiviral infection of pCDH-DEPTOR evidently accelerated HPB-ALL cell proliferation (Figure 4e) and, more importantly, rescued NOTCH1-dependent HPB-ALL from NOTCH pathway inhibition (Supplementary Figure S4d). In addition, DEPTOR overexpression significantly increased glucose uptake and lactate secretion, and also rescued suppression of glycolysis by Compound E (Figure 4f).[29] These loss- and gain-of-function studies provide compelling evidence supporting that DEPTOR is a critical mediator

downstream of NOTCH1 in promoting T-ALL cell proliferation, survival and glycolysis.

**DEPTOR ablation delays T-ALL onset in a xenograft model**

To understand the role of DEPTOR *in vivo*, five million HPB-ALL cells with or without DEPTOR expression were intravenously injected into immuno-compromised NOD-Scid-IL2Rγ$^{-/-}$ (NSI) mice (Figure 5a).[37,38] After 25 days post engraftment, the control cohort
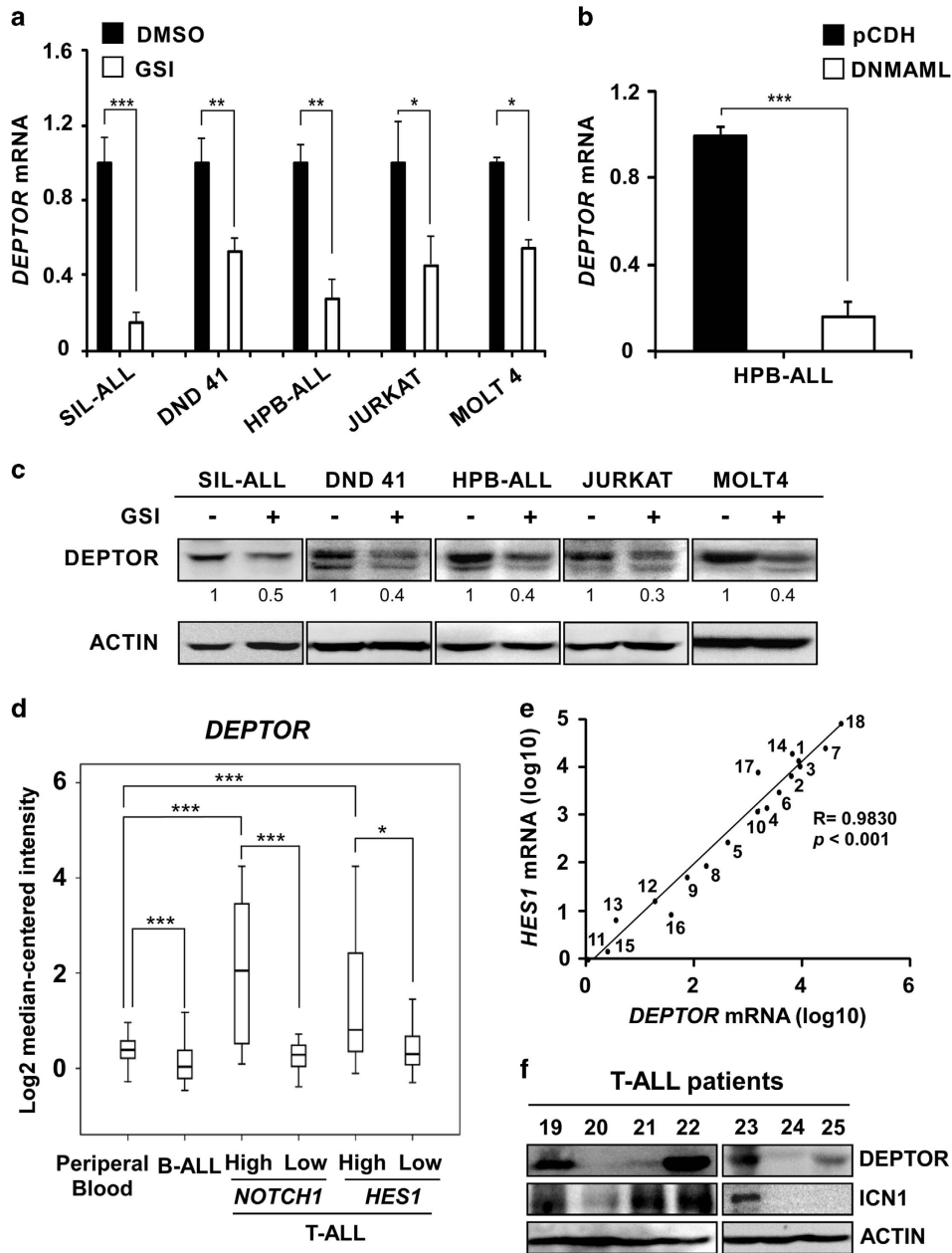
Figure 2. DEPTOR expression is regulated by NOTCH1 signaling in human T-ALL. (**a**–**c**) DEPTOR expression is downregulated by NOTCH1 inhibition in human T-ALL cells. *DEPTOR* mRNA was quantified in human T-ALL cells upon Compound E (1 μM) treatment for 48 h in **a** or dominant negative MAML (DNMAML) expression in **b**. Data were presented as the mean values ($\pm$ s.d.) of triplicates. DEPTOR proteins were analyzed and quantified after 48 h Compound E (1 μM) or DMSO treatment as shown in **c**. (**d**) *DEPTOR* expression was highly correlated with NOTCH1 activity in primary T-ALLs. *DEPTOR* mRNA levels were assessed in microarray data (GSE13204) from Haferlach *et al*. PB: normal peripheral blood. For more details, please see Supplementary Figure S2. (**e**) Correlation between *DEPTOR* and *HES1* mRNA levels. Eighteen primary T-ALL cDNA samples obtained from Tongji Hospital and Jiangsu Institute of Hematology were used for the analysis. (**f**) Immunoblot analysis of DEPTOR, ICN1 and ACTIN proteins. Seven primary T-ALL samples provided by Tongji Hospital were used. *$P < 0.05$, **$P < 0.01$ and ***$P < 0.001$.

exhibited characteristic leukemia phenotypes and started to decease. In contrast, DEPTOR shRNA-expressing mice had significantly prolonged lifespans (Figure 5b). Physical findings in the deceased control mice included splenomegaly, yet the DEPTOR-depleted cohorts which were simultaneously killed had much smaller spleen sizes (Figure 5c). Flow cytometric analysis revealed marked accumulation of human CD45^{+} leukemia cells in the spleen, bone marrow and peripheral blood from the control mice, manifesting these animals were sick and dead due to

dissemination of human T-ALL cells. In contrast, much fewer human CD45^{+} cells were detected in the DEPTOR-depleted mice (Figures 5d and e). Histological analysis further confirmed that less proliferation of human leukemia cells was detected in mice engrafted with DEPTOR-depleted cells, as evidenced by attenuated CD45 and PCNA staining (Figure 5f) and hematoxylin and eosin staining (Supplementary Figure S5). These findings support that DEPTOR has a vital role in T-ALL development *in vivo*.
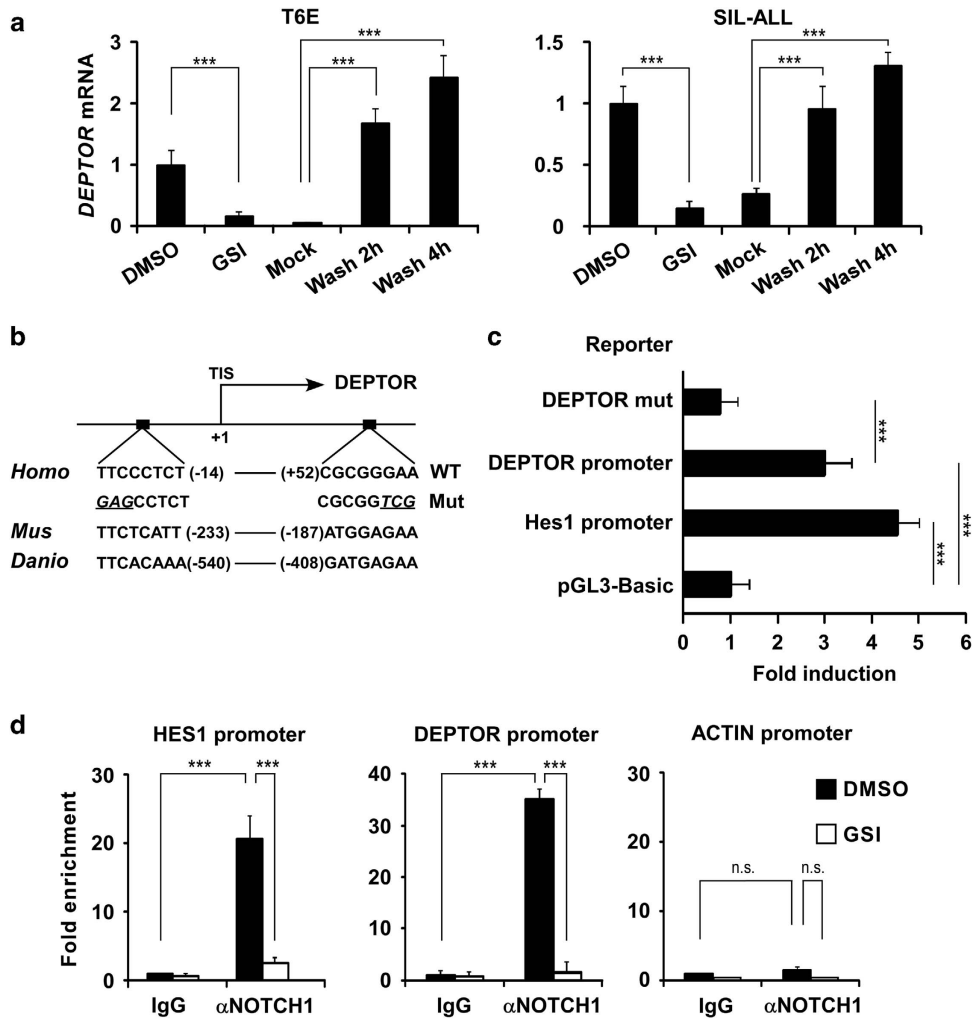
Figure 3. NOTCH1 directly binds to the *DEPTOR* promoter and activates its transcription. (**a**) T6E or SIL-ALL cells were treated with Compound E (1 μM) for 48 h then washed and refed with medium containing Compound E (mock), or medium lacking Compound E (wash). RNA levels were determined by qRT-PCR. (**b**) Schematic presentation of two CSL-binding sites proximal to the *DEPTOR* promoter revealed in various species. TIS, +1 transcription initiation site; WT, wild type; Mut, mutant. (**c**) 293T cells were co-transfected with pGL3 luciferase reporter constructs and ICN1 expressing plasmids. Luciferase reporter activities normalized with pGL3-Basic vector were determined and presented as fold induction, shown as the average of triplicates. (**d**) Physical association of ICN1 with the *DEPTOR*, *HES1* and *ACTIN* promoters was detected by chromatin immunoprecipitation in SIL-ALL cells using a specific NOTCH1 antibody (αNOTCH1) or isotype control IgG. *$P < 0.05$, **$P < 0.01$ and ***$P < 0.001$. n.s. means non-significant. qRT-PCR, quantitative real-time PCR.

DEPTOR activates AKT in T-ALL

We next sought to understand whether DEPTOR is an essential player downstream of NOTCH1 in mediation of AKT activation. To this end, we depleted DEPTOR expression in HPB-ALL cells and followed AKT activity reflected by phosphorylations at the Serine 473 and Threonine 308 residues. As shown in Figure 6a and Supplementary Figure S6a, DEPTOR-depleted cells exhibited much weaker AKT phosphorylation. Of note, DEPTOR-depleted cells that were retrieved back from the animals consistently displayed reduced AKT phosphorylation at both residues (Figure 6a). Moreover, overexpression of DEPTOR elevated AKT activation and, strikingly, reversed inhibitory effects on AKT phosphorylation by Compound E (Figure 6b). In contrast, the phosphorylation-defective DEPTOR mutant ($13 \times S/T \rightarrow A$) failed to induce AKT (Figure 6b). Consistent with previous findings,[20] we found that DEPTOR depletion increased S6K1 phosphorylation while its overexpression inhibited S6K1 phosphorylation (Supplementary Figure S6b), suggesting that DEPTOR activates AKT in part through inhibiting mTORC1 activity. Nevertheless, we cannot exclude possibilities that additional mechanisms may contribute to AKT

activation. When applying a specific AKT inhibitor MK2206 in DEPTOR-overexpressing HPB-ALL cells, not only AKT phosphorylation was completely abolished (Figure 6c), but DEPTOR-mediated growth advantages were also diminished (Figure 6d). We thus conclude DEPTOR-mediated AKT activation accounts for accelerated cell expansion and these findings support a model that NOTCH1 regulates multiple downstream targets to activate AKT (Figure 6e).

DISCUSSION

The biological functions of DEPTOR in tumorigenesis remain obscure as DEPTOR could be either oncogenic or tumor-suppressive depending on specific cellular contexts and tumor types.[20] In this study, we establish a vital role of DEPTOR in contribution to T-cell leukemogenesis. Transcriptionally regulated by oncogenic NOTCH1, DEPTOR expression profoundly enhances AKT activation. Notably, AKT inhibition completely abrogates the function of DEPTOR in promoting cell proliferation. Our findings not only decipher a novel mechanism how DEPTOR is
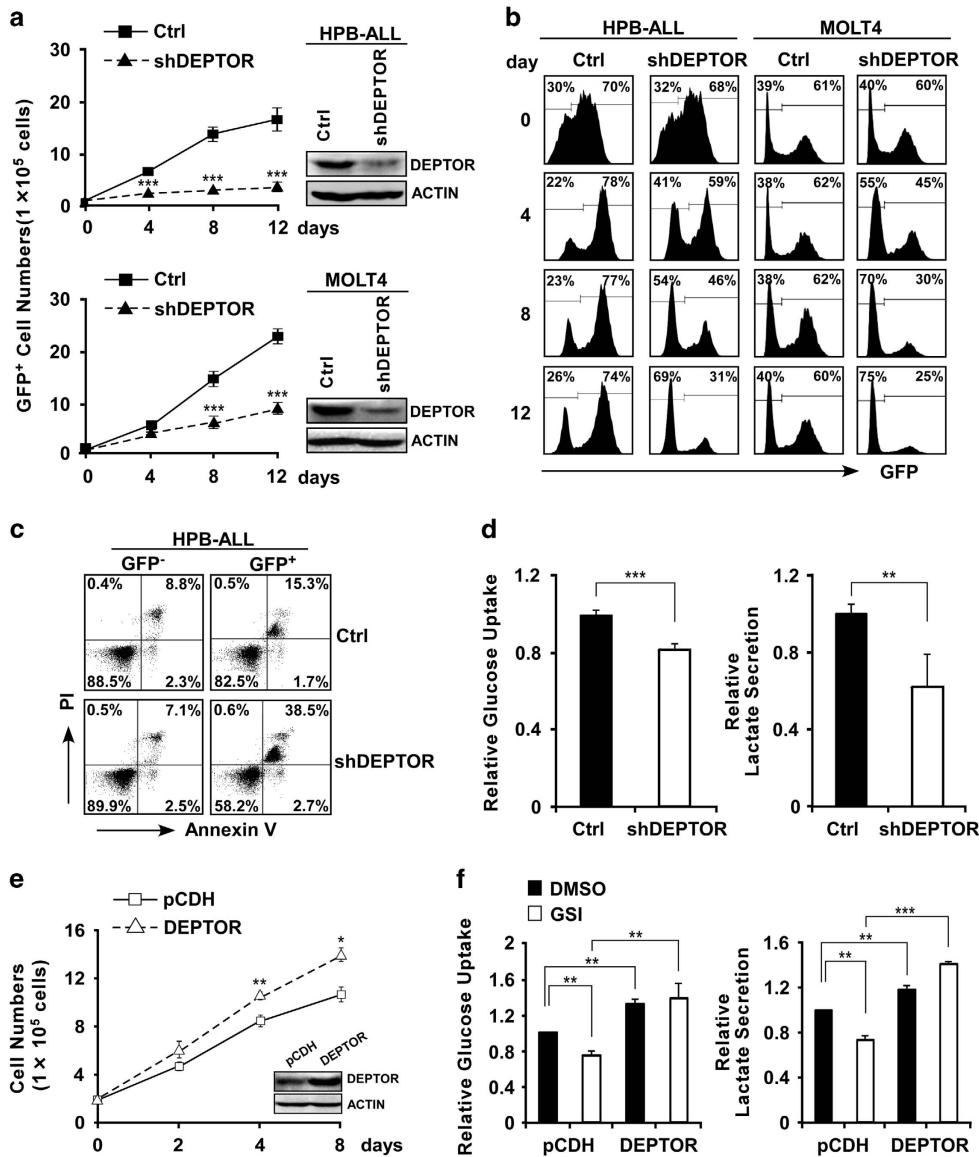
Figure 4. DEPTOR promotes T-ALL cell proliferation, survival and aerobic glycolysis. (**a**) DEPTOR depletion slowed down T-ALL cell growth. shRNA targeting *DEPTOR* was introduced into the pLKO.1 vector with a surrogated GFP marker and used for lentivirus preparation. HPB-ALL or MOLT4 cells were infected with the indicated lentivirus and DEPTOR expression was assessed by immunoblotting from sorted GFP+ population 4 days post infection. Live GFP+ cell numbers were counted and plotted. (**b**) Unsorted cells were alternatively analyzed for GFP+ percentages 2 days post infection by flow cytometry. (**c**) Apoptotic cell death of HPB-ALL as shown in **b** was detected by PI-Annexin V staining 8 days post infection. (**d**) Glucose uptake and lactate secretion normalized to the same number of live GFP+ HPB-ALL cells were examined 48 h post infection. (**e**) HPB-ALL cells were infected with lentiviruses expressing pCDH or pCDH-DEPTOR, cultured for 2 days and then selected with puromycin (1 μg/ml) for additional 48 h. DEPTOR expression was assessed by immunoblotting. Live cells were counted at indicated time points. (**f**) Relative glucose uptake and lactate release were examined 48 h after DMSO or Compound E (1 μM) treatment in puromycin-selected HPB-ALL cells. Data were normalized to the same number of live cells. Error bars represent means ± s.d. of triplicate experiments. Ctrl, control shRNA targeting luciferase. *$P < 0.05$, **$P < 0.01$ and ***$P < 0.001$.

transcriptionally regulated but also reveal an alternative mechanism for AKT deregulation, establishing DEPTOR as a bridge linking the crosstalk between NOTCH1 and AKT in T-cell transformation.

Our studies have provided mechanistic insights in how *DEPTOR* is regulated in T-ALL and determined its crucial role in leukemogenesis. In contrast to protein stability uniformly regulated by Casein kinase I-mediated phosphorylation and subsequent polyubiquitination by the SCF$^{\beta\text{-TrCP}}$ E3 ligase,[39–41] transcriptional control of *DEPTOR* seems much more complex, being highly tissue-specific and context-dependent.[20,22,23,42] In T-cell leukemia, we have provided lines of evidence demonstrating transcriptional control of *DEPTOR* by NOTCH1 (Figures 1–3)

and generally shown positive correlations between NOTCH1 and DEPTOR in primary T-ALL samples (Figures 2d–f). Yet exceptions do exist; in some primary specimens, DEPTOR is expressed, whereas cleaved NOTCH1 is undetectable (Figure 2f). These results suggest that additional mechanisms are also implicated in modulation of DEPTOR expression in T-ALL (for example, regulation of protein stability).

Our data suggest that DEPTOR acts as an important player in the pathogenesis of T-cell leukemia. In support of this notion, DEPTOR-ablated T-ALL cells expanded less efficiently *in vivo* and mice bearing these cells exhibited prolonged survival (Figure 5b). Given enforced expression of DEPTOR promoted HPB-ALL cell
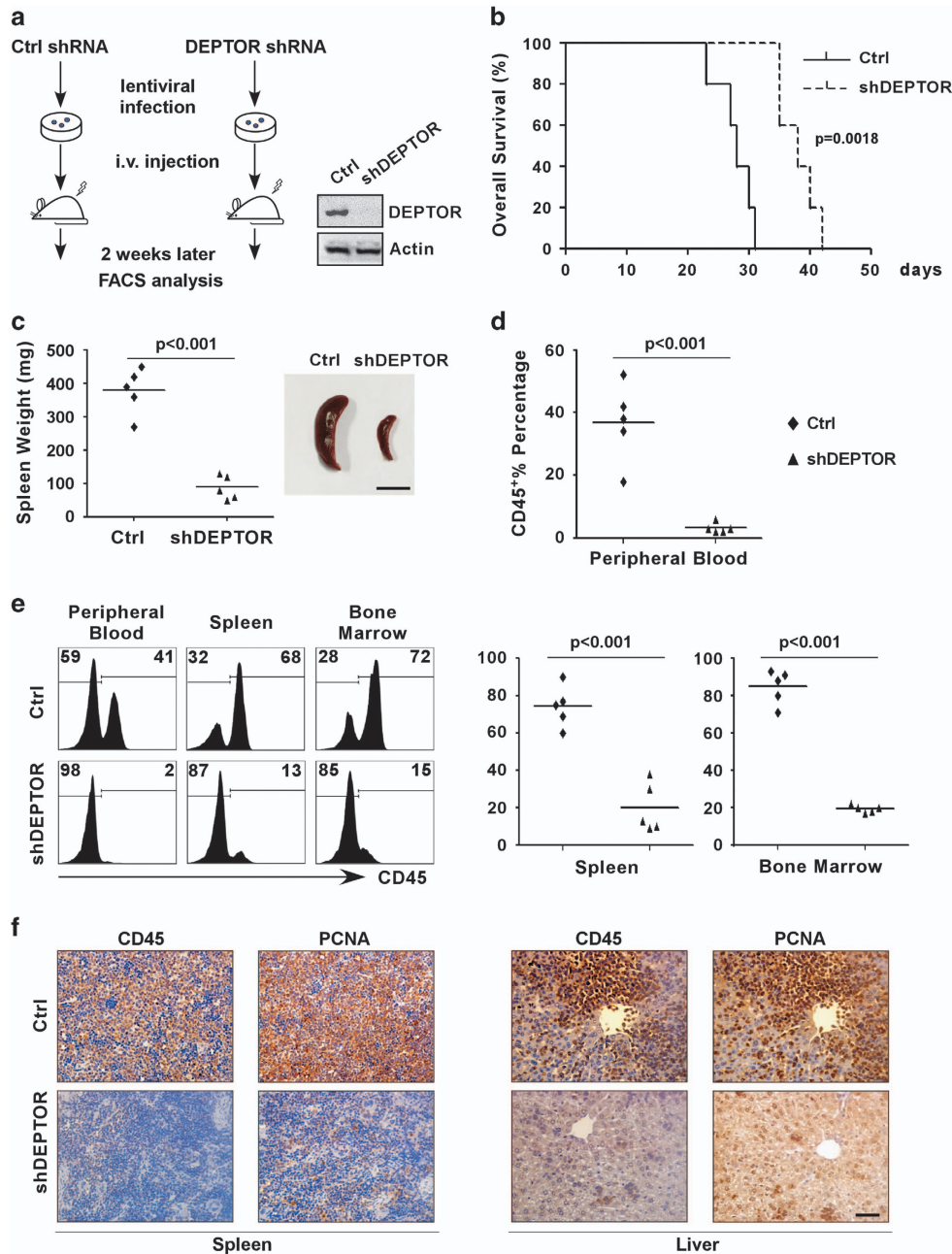
Figure 5. DEPTOR depletion slows down T-ALL onset *in vivo*. (**a**) Schematic representation of the xenograft model. HPB-ALL cells were infected with lentiviruses expressing PLKO.1-Ctrl (shRNA targeting luciferase as control) or PLKO.1-shDEPTOR (shDEPTOR). Two days post infection, cells were subjected to puromycin (1 μg/ml) selection for 48 h, followed by immunoblotting of DEPTOR shown on the right. Resulting live cells were intravenously injected into immuno-compromised NSI mice (for more details, see materials and methods). (**b**) Kaplan–Meier survival curves of mice injected with HPB-ALL cells expressing a control shRNA (Ctrl, $n = 5$) or DEPTOR shRNA (shDEPTOR, $n = 5$). Statistic significance was calculated with log-rank test (GraphPad Prism). (**c**, left) Spleen weights at ~30 days post injection ($n = 5$ in each group). (right) Representative spleen images. Scale bar, 1 cm. (**d**) Human CD45$^+$ cells, representing engrafted tumor burden, were analyzed in peripheral blood, spleen and bone marrow from denoted groups. (**e**) Representative flow cytometric plots from **d** were shown. (**f**) Representative immunohistological images of human CD45 and human PCNA in spleen and liver sections from the control and shDEPTOR mice. Scale bar, 50 μm.

proliferation *in vitro* (Figure 3e), we also assessed whether ectopically expressed DEPTOR could enhance leukemogenesis *in vivo*. Unexpectedly, overexpression of DEPTOR in HPB-ALL cell barely accelerated T-cell leukemogenesis (Supplementary Figure S7), suggesting that DEPTOR activity is necessary but not sufficient for T-ALL development *in vivo*. Albeit significantly delayed, mice injected with DEPTOR-depleted cells eventually succumbed to leukemia (Figure 5b). This observation raises the possibility that

T-ALL cells may ultimately escape DEPTOR dependency. To test this, we performed a time course analysis of cell survival upon DEPTOR depletion in HPB-ALL cells *in vitro* and found that DEPTOR inhibition gradually increased cell death from day 2 to day 12. However, as the culture continued, the death-promoting effect by DEPTOR knockdown progressively diminished even though DEPTOR was still largely silenced (Supplementary Figure S8). These findings suggest that, when DEPTOR is inhibited in T-ALL,
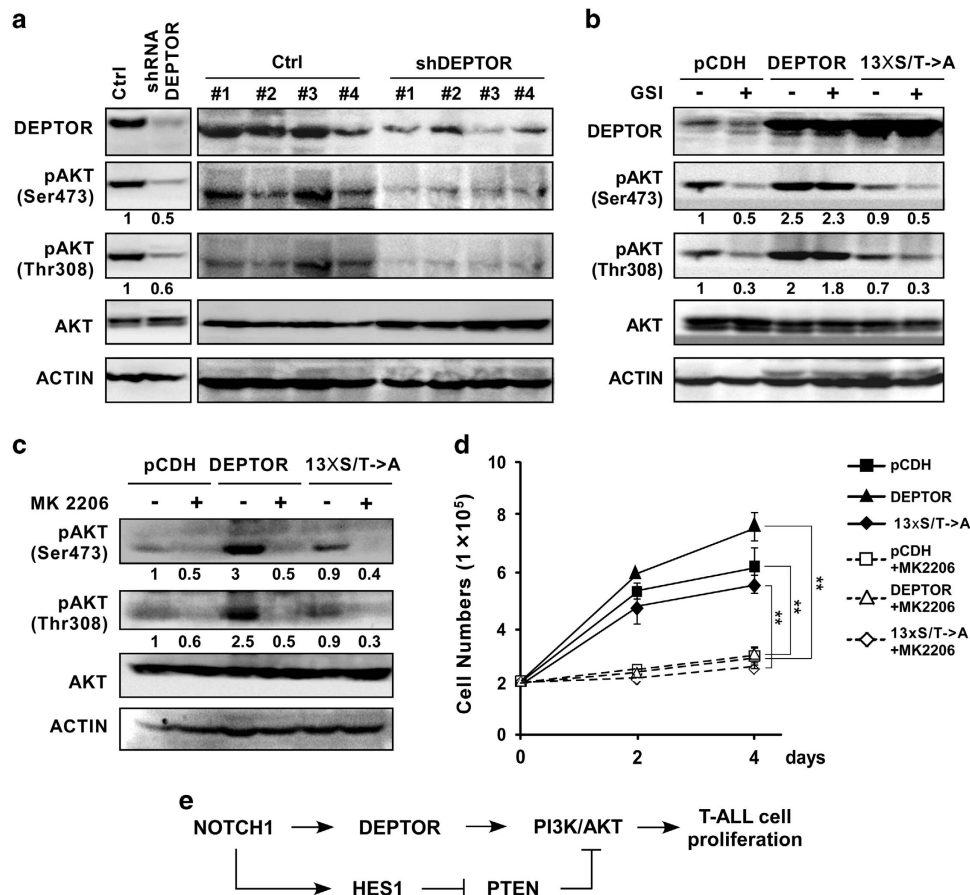
Figure 6. DEPTOR promotes T-ALL cell proliferation via AKT activation. (**a**) Immunoblots of total protein lysates from HPB-ALL cells infected with indicated lentiviruses as well as total protein lysates of HPB-ALL cells (sorted by human CD45 staining) retrieved back from mice as shown in Figure 5. (**b**) Control or DEPTOR-expressing HPB-ALL cells were treated with or without Compound E (1 μM) for 72 h and total cellular lysates were subjected to immunoblot assays using indicated antibodies. (**c**) HPB-ALL cells were transduced with lentiviruses expressing indicated proteins and purified by puromycin (1 μg/ml) selection, treated with or without AKT inhibitor MK2206 (1 μM) for 48 h. Total cellular lysates were subjected to immunoblot assays using indicated antibodies. (**d**) Infected and purified HPB-ALL cells expressing respective proteins as shown in **c** were cultured in the presence or absence of MK2206 (1 μM) for 2 and 4 days. Live cells were counted and plotted. $**P < 0.01$. (**e**) Transcriptional network downstream of NOTCH1 that controls AKT activation and cellular functions in T-ALL.

cells may eventually acquire resistance through alternative mechanisms. Therefore, one must use caution when considering DEPTOR antagonists as potential therapeutics for T-ALL treatment.

AKT activation has emerged as another critical effector in the pathogenesis of T-ALL. PTEN-inactivating mutations[29] or micro-deletions[43] are found in a subset of T-ALLs, leading to constitutive AKT activation. Of note, in PTEN wild-type T-ALL, AKT is frequently activated through other mechanisms. Palomero *et al.*[29] previously reported NOTCH1-mediated AKT activation through the canonical target *HES1*. Our data provide an alternative mechanism that *DEPTOR*, another important down-stream target, mediates NOTCH1 regulation of AKT and promotes T-cell leukemogenesis. It is conceivable that NOTCH1 applies a variety of means to activate AKT that is required for multiple oncogenic processes (Figure 6e). Our findings nevertheless highlight DEPTOR as a pivotal player in T-ALL and also provide additional molecular basis for administration of AKT inhibitors in T-ALL treatment.

MATERIALS AND METHODS

Cell lines and reagents

T-ALL cells were maintained in RPMI-1640 supplemented with 10% fetal bovine serum, antibiotics (Hyclone, Logan, UT, USA), 2 mM L-glutamine,

1 mM sodium pyruvate, 1% non-essential amino acids and β-mercap-toethanol (Sigma, St Louis, MO, USA). T6E, SIL-ALL, HPB-ALL and DND41 cells were kindly provided by Dr Warren Pear at the University of Pennsylvania, PA, USA and maintained as previously described.[9,10] 293T, MOLT4 and JURKAT cells were purchased from American Type Culture Collection (ATCC, Manassas, VA, USA). All cell lines were cultured for fewer than 6 months after resuscitation and tested for mycoplasma contamina-tion using the MycoAlert Mycoplasma Detection kit (Lonza, Slough, UK). Primary T-ALL cDNAs or protein lysates were obtained from the Department of Hematology, Tongji Hospital, Wuhan and Jiangsu Institute of Hematology, Suzhou, People's Republic of China. Studies using these specimens were approved by the Clinical Research Ethics Committee of Tongji Medical College, Huazhong University of Science and Technology [2014]IEC(S013) and informed consent was obtained. Compound E, DAPT and MK2206 were purchased from Merck (Kenilworth, NJ, USA), Sigma (St Louis, MO, USA). and Selleck Chemicals LLC (Houston, TX, USA), respectively.

Expression profiling and analysis

T6E cells were treated with 1 μM DAPT for 12 h and total RNAs were prepared using TRIzol (Invitrogen, Carlsbad, CA, USA). Total RNAs were labeled as cRNAs and hybridized on Affymetrix GeneChip Mouse Genome 430 2.0. Arrays were then scanned on an Affymetrix GeneChip scanner according to the protocol from Shanghai Biotechnology Corporation (Shanghai, People's Republic of China). The raw data were normarlized using 3′ Expression Arrays-RMA method by Expression console (Affymetrix,

Santa Clara, CA, USA). Genes with fold changes (GSI versus DMSO) > 1.3 or < -1.3 were selected for further analysis.

Lentiviral transduction

Lentiviral vectors PLKO.1 encoding a shRNA targeted against DEPTOR, or pCDH vectors expressing DEPTOR or mutant ($13 \times S/T \rightarrow A$, Addgene, Cambridge, MA, USA), were constructed and transfected into 293T simultaneously with helper plasmids (pMD2.G and psPAX2). Viral supernatants were collected for infection, then supplemented with 8 μg/ml polybrene and centrifuged for 1.5 h at room temperature before 24 h incubation.[44] The sequences for DEPTOR shRNAs were shDEPTOR, 5′-GCAA GGAAGACATTCACGATT-3′[20] or shDEPTOR#1, 5′-GCACCTTCATGGCATCTG AAT-3′. Primers used to clone DEPTOR were 5′-ATGCTCTAGAGCCACC ATGGAGGAGGGCGGCAGCA-3′ (forward) and 5′-CGATGGATCCTCAGCACT CTAACTCCTCCATG-3′ (reverse).

Glucose uptake and lactate secretion assays

Glucose uptake or lactate secretion analysis was carried out using respective Colorimetric Assay Kits (BioVision, Milpitas, CA, USA). In brief, 4×10^5 cells were seeded in six-well plates and cultured for 48 h. Culture medium were then collected to quantify glucose and lactate. Consumed glucose and released lactate were calculated and normalized to the same cell numbers.

RNA extraction and quantitative real-time PCR

Total RNA was extracted using TRIzol (Invitrogen). Random primed total RNAs (1 μg) were reverse-transcribed with RevertAid First strand cDNA synthesis kit according to the manufacturer's instructions (Thermo Scientific, Waltham, MA, USA). Quantitative PCR was conducted using FAST SYBR Green Master Mix on CFX Connect Real-Time PCR System (Bio-Rad, Hercules, CA, USA). Relative expression of the mRNA was calculated using the $2^{-\Delta\Delta Ct}$ method.[9] Primer sequences were as following: human DEPTOR forward, 5′-CACCATGTGTGTGATGAGCA-3′; reverse, 5′-GGCCTTCACTTCATTATCCAA-3′; mouse Deptor forward, 5′-ACAAG CCTTCCTGGTGGTTC-3′; reverse, 5′-CTTTTCTTCATGGAGCCGCAG-3′; human HES1 forward, 5′-TCAACACGACACCGGATAAA-3′; reverse, 5′-TCAGCTGG CTCAGACTTTC A-3′; human and mouse 18s RNA forward, 5′-GCGCC GCTAGAGGTGAAAT-3′; reverse, 5′-GGCGGGTCATGGGAATAAC-3′.

Western blot analysis

Cells were lysed in RIPA (50 mM Tris-HCl pH7.4, 150 mM NaCl, 1% TritonX-100, 1% sodium deoxycholate, 0.1% SDS, 2 mM sodium pyrophosphate, 25 mM β-glycerophosphate, 1 mM EDTA, 1 mM Na_3VO_4 and 0.5 μg/ml leupeptin).[45] Fifty microgram total cellular proteins were subjected to SDS–polyacrylamide gel and transferred to PVDF membrane, which was blocked with 5% nonfat milk, and incubated with the primary antibodies overnight at 4 °C. Appropriate horseradish peroxidase-conjugated secondary antibodies were applied for 1 h at room temperature before detection with an enhanced chemiluminescence kit (Thermo Scientific). Densitometric analyses of protein abundance were determined by Image J software (Bethesda, MD, USA). Antibodies against DEPTOR (49674) and β-ACTIN (47778) were purchased from Novus Biologicals (Littleton, CO, USA) and Santa Cruz Biotechnology (Dallas, TX, USA). Antibodies from Cell Signaling Technology (Danvers, MA, USA) include phospho- AKT-Ser473 (4060), phospho-AKT-Thr308 (2965) and pan-AKT (4691).

Chromatin immunoprecipitation assay

Chromatin immunoprecipitation was performed as described.[10] Briefly, SIL-ALL cells were treated with DMSO or Compound E (1 μM) for 72 h then fixed with 1% paraformaldehyde at room temperature for 10 min. Precleared chromatin was immunoprecipitated with antiserum against NOTCH1 for 16 h and protein G agarose/salmon sperm DNA beads (Millipore, Billerica, MA, USA) for 1 h at 4 °C. The eluted material was reverse-cross-linked and treated with proteinase K. DNA was purified by phenol/chloroform extraction, eluted by distilled H_2O and quantified by CFX Connect Real-Time PCR System (Bio-Rad) using specific primers. HES1 promoter: forward, 5′-CGTGTCTCCTCCTCCCATT-3′; reverse, 5′-CGGATCC TGTGTGATCCCTA-3′; DEPTOR promoter: forward, 5′-ATTCCCTCTCCAGCCA ATCC-3′; reverse, 5′-TCCATGGTTTTAGGGCCGTG-3′; ACTIN promoter: forward, 5′-GACTTCTAAGTGGCCGCAAG-3′; reverse, 5′-TTGCCGACTTCAGAGCAAC-3′.

Luciferase reporter assay

pGL3-basic vector expressing the DEPTOR promoter was constructed using primers: forward, 5′-ATCGGGTACCCCATAGGGATTCCCTCTCCAGC-3′; reverse, 5′-TACGCTCGAGGCCCTCACAGACGCTTCCCGCG-3′. Mutant DEPTOR promoter was amplified with primers: forward, 5′-ATCGGGTACCCCATAGGGAGAGC CTCTCCAGC-3′; reverse, 5′-TACGCTCGAGGCCCTCACAGACGCCGACCGCG-3′. To detect luciferase reporter activity, empty pGL3-basic firefly luciferase vector (0.8 μg) or pGL3 expressing the DEPTOR promoter (or indicated mutants) and 0.2 μg pcDNA3-ICN1 plasmid, along with 50 ng Renilla luciferase reporter construct, were co-transfected into 293T cells using Lipofectamine 2000 (Invitrogen). Luciferase activities were measured 24 h later using Dual Luciferase Reporter Assay System (Promega, Madison, WI, USA).[9] Firefly luciferase activities were normalized with Renilla luciferase control values. Relative activity from the empty vector lysate was set arbitrarily to a value of 1.

Flow cytometry

Cells with GFP fluorescence or stained with indicated antibodies were resuspended in phosphate-buffered saline buffer. Acquisition was performed on an Accuri C6 (BD Biosciences, Franklin Lakes, NJ, USA). Dead cells and doublets were excluded based on FSC-W and SSC-W characteristics. Data were analyzed with FlowJo software (Tree Star, Ashland, OR, USA).

T-ALL xenografts

A total of 5×10^6 HPB-ALL cells, transduced with lentiviruses encoding pLKO.1-puro-shLUC or pLKO.1-puro-shDEPTOR, were injected intravenously into one of the randomized 6-week-old female irradiated (1 Gy) NOD-SCID $IL2Rg^{-/-}$ (NSI) mice (Guangzhou Institutes of Biomedicine and Health, GIBH, Guangzhou, People's Republic of China). Mice were inspected three times weekly to detect early signs and symptoms of leukemia by two investigators who were blinded to group allocation. T-ALL cell engraftment was monitored by flow cytometric analysis of human CD45 expression. Animal experiments were performed in the Laboratory Animal Center of GIBH and all animal procedures were approved by the Animal Welfare Committee of GIBH.

Immunohistochemistry

The immunohistological analysis was carried out using Histostain-Plus IHC Kit (Invitrogen) as described.[46] Spleen or liver sections were stained with antibodies against human CD45 (13–9457, eBioscience, San Diego, CA, USA) or human PCNA (sc-56, Santa Cruz Biotechnology) overnight at 4 °C, then subjected to incubation with biotinylated secondary antibodies for 30 min and horseradish peroxidase-linked streptavidin agents for 15 min at room temperature. Stains were visualized by the DAB substrate kit (Vector Labs, Burlingame, CA, USA).

Statistical analysis

Data are presented as means ± s.d. Student's *t*-test was used in all significance analysis except that Wilcoxon signed-rank test and log-rank test were applied in patient samples and animal experiments, respectively. $P < 0.05$ is considered statistically significant.

REFERENCES

1 Van Vlierberghe P, Ferrando A. The molecular basis of T cell acute lymphoblastic leukemia. *J Clin Invest* 2012; **122**: 3398–3406.

2 Pui CH, Evans WE. Treatment of acute lymphoblastic leukemia. *N Engl J Med* 2006; **354**: 166–178.

3 Weng AP, Ferrando AA, Lee W, Morris JPT, Silverman LB, Sanchez-Irizarry C *et al.* Activating mutations of NOTCH1 in human T cell acute lymphoblastic leukemia. *Science* 2004; **306**: 269–271.

4 O'Neil J, Grim J, Strack P, Rao S, Tibbitts D, Winter C *et al.* FBW7 mutations in leukemic cells mediate NOTCH pathway activation and resistance to gamma-secretase inhibitors. *J Exp Med* 2007; **204**: 1813–1824.

5 Thompson BJ, Buonamici S, Sulis ML, Palomero T, Vilimas T, Basso G *et al.* The SCFFBW7 ubiquitin ligase complex as a tumor suppressor in T cell leukemia. *J Exp Med* 2007; **204**: 1825–1835.

6 Paganin M, Ferrando A. Molecular pathogenesis and targeted therapies for NOTCH1-induced T-cell acute lymphoblastic leukemia. *Blood Rev* 2011; **25**: 83–90.

7 Kopan R, Ilagan MX. The canonical Notch signaling pathway: unfolding the activation mechanism. *Cell* 2009; **137**: 216–233.

8 Taipale M, Jarosz DF, Lindquist S. HSP90 at the hub of protein homeostasis: emerging mechanistic insights. *Nat Rev Mol Cell Biol* 2010; **11**: 515–528.

9 Liu H, Chi AW, Arnett KL, Chiang MY, Xu L, Shestova O *et al.* Notch dimerization is required for leukemogenesis and T-cell development. *Genes Dev* 2010; **24**: 2395–2407.

10 Weng AP, Millholland JM, Yashiro-Ohtani Y, Arcangeli ML, Lau A, Wai C *et al.* c-Myc is an important direct target of Notch1 in T-cell acute lymphoblastic leukemia/lymphoma. *Genes Dev* 2006; **20**: 2096–2109.

11 Connell P, Ballinger CA, Jiang J, Wu Y, Thompson LJ, Hohfeld J *et al.* The co-chaperone CHIP regulates protein triage decisions mediated by heat-shock proteins. *Nat Cell Biol* 2001; **3**: 93–96.

12 Dohda T, Maljukova A, Liu L, Heyman M, Grander D, Brodin D *et al.* Notch signaling induces SKP2 expression and promotes reduction of p27Kip1 in T-cell acute lymphoblastic leukemia cell lines. *Exp Cell Res* 2007; **313**: 3141–3152.

13 Margolin AA, Palomero T, Sumazin P, Califano A, Ferrando AA, Stolovitzky G. ChIP-on-chip significance analysis reveals large-scale binding and regulation by human transcription factor oncogenes. *Proc Natl Acad Sci USA* 2009; **106**: 244–249.

14 Medyouf H, Gusscott S, Wang H, Tseng JC, Wai C, Nemirovsky O *et al.* High-level IGF1R expression is required for leukemia-initiating cell activity in T-ALL and is supported by Notch signaling. *J Exp Med* 2011; **208**: 1809–1822.

15 Real PJ, Tosello V, Palomero T, Castillo M, Hernando E, de Stanchina E *et al.* Gamma-secretase inhibitors reverse glucocorticoid resistance in T cell acute lymphoblastic leukemia. *Nat Med* 2009; **15**: 50–58.

16 Roti G, Carlton A, Ross KN, Markstein M, Pajcini K, Su AH *et al.* Complementary genomic screens identify SERCA as a therapeutic target in NOTCH1 mutated cancer. *Cancer Cell* 2013; **23**: 390–405.

17 Schnell SA, Ambesi-Impiombato A, Sanchez-Martin M, Belver L, Xu L, Qin Y *et al.* Therapeutic targeting of HES1 transcriptional programs in T-ALL. *Blood* 2015; **125**: 2806–2814.

18 Wang H, Zang C, Taing L, Arnett KL, Wong YJ, Pear WS *et al.* NOTCH1-RBPJ complexes drive target gene expression through dynamic interactions with superenhancers. *Proc Natl Acad Sci USA* 2014; **111**: 705–710.

19 Wang H, Zou J, Zhao B, Johannsen E, Ashworth T, Wong H *et al.* Genome-wide analysis reveals conserved and divergent features of Notch1/RBPJ binding in human and murine T-lymphoblastic leukemia cells. *Proc Natl Acad Sci USA* 2011; **108**: 14908–14913.

20 Peterson TR, Laplante M, Thoreen CC, Sancak Y, Kang SA, Kuehl WM *et al.* DEPTOR is an mTOR inhibitor frequently overexpressed in multiple myeloma cells and required for their survival. *Cell* 2009; **137**: 873–886.

21 Bruneau S, Nakayama H, Woda CB, Flynn EA, Briscoe DM. DEPTOR regulates vascular endothelial cell activation and proinflammatory and angiogenic responses. *Blood* 2013; **122**: 1833–1842.

22 Laplante M, Horvat S, Festuccia WT, Birsoy K, Prevorsek Z, Efeyan A *et al.* DEPTOR cell-autonomously promotes adipogenesis, and its expression is associated with obesity. *Cell Metab* 2012; **16**: 202–212.

23 Meng ZX, Li S, Wang L, Ko HJ, Lee Y, Jung DY *et al.* Baf60c drives glycolytic metabolism in the muscle and improves systemic glucose homeostasis through Deptor-mediated Akt activation. *Nat Med* 2013; **19**: 640–645.

24 Zhang H, Chen J, Zeng Z, Que W, Zhou L. Knockdown of DEPTOR induces apoptosis, increases chemosensitivity to doxorubicin and suppresses autophagy in RPMI-8226 human multiple myeloma cells in vitro. *Int J Mol Med* 2013; **31**: 1127–1134.

25 Zhang HR, Chen JM, Zeng ZY, Que WZ. Knockdown of DEPTOR inhibits cell proliferation and increases chemosensitivity to melphalan in human multiple myeloma RPMI-8226 cells via inhibiting PI3K/AKT activity. *J Int Med Res* 2013; **41**: 584–595.

26 Proud CG. Dynamic balancing: DEPTOR tips the scales. *J Mol Cell Biol* 2009; **1**: 61–63.

27 Wang Z, Zhong J, Inuzuka H, Gao D, Shaik S, Sarkar FH *et al.* An evolving role for DEPTOR in tumor development and progression. *Neoplasia* 2012; **14**: 368–375.

28 Palomero T, Dominguez M, Ferrando AA. The role of the PTEN/AKT Pathway in NOTCH1-induced leukemia. *Cell Cycle* 2008; **7**: 965–970.

29 Palomero T, Sulis ML, Cortina M, Real PJ, Barnes K, Ciofani M *et al.* Mutational loss of PTEN induces resistance to NOTCH1 inhibition in T-cell leukemia. *Nat Med* 2007; **13**: 1203–1210.

30 Palomero T, Ferrando A. Oncogenic NOTCH1 control of MYC and PI3K: challenges and opportunities for anti-NOTCH1 therapy in T-cell acute lymphoblastic leukemias and lymphomas. *Clin Cancer Res* 2008; **14**: 5314–5317.

31 Piovan E, Yu J, Tosello V, Herranz D, Ambesi-Impiombato A, Da Silva AC *et al.* Direct reversal of glucocorticoid resistance by AKT inhibition in acute lymphoblastic leukemia. *Cancer Cell* 2013; **24**: 766–776.

32 Pear WS, Aster JC, Scott ML, Hasserjian RP, Soffer B, Sklar J *et al.* Exclusive development of T cell neoplasms in mice transplanted with bone marrow expressing activated Notch alleles. *J Exp Med* 1996; **183**: 2283–2291.

33 Haferlach T, Kohlmann A, Wieczorek L, Basso G, Kronnie GT, Bene MC *et al.* Clinical utility of microarray-based gene expression profiling in the diagnosis and subclassification of leukemia: report from the International Microarray Innovations in Leukemia Study Group. *J Clin Oncol* 2010; **28**: 2529–2537.

34 Khwaja SS, Liu H, Tong C, Jin F, Pear WS, van Deursen J *et al.* HIV-1 Rev-binding protein accelerates cellular uptake of iron to drive Notch-induced T cell leukemogenesis in mice. *J Clin Invest* 2010; **120**: 2537–2548.

35 Herranz D, Ambesi-Impiombato A, Palomero T, Schnell SA, Belver L, Wendorff AA *et al.* A NOTCH1-driven MYC enhancer promotes T cell development, transformation and acute lymphoblastic leukemia. *Nat Med* 2014; **20**: 1130–1137.

36 Lu B, Sun X, Chen Y, Jin Q, Liang Q, Liu S *et al.* Novel function of PITH domain-containing 1 as an activator of internal ribosomal entry site to enhance RUNX1 expression and promote megakaryocyte differentiation. *Cell Mol Life Sci* 2015; **72**: 821–832.

37 Xiao Y, Jiang Z, Li Y, Ye W, Jia B, Zhang M *et al.* ANGPTL7 regulates the expansion and repopulation of human hematopoietic stem and progenitor cells. *Haematologica* 2015; **100**: 585–594.

38 Ye W, Jiang Z, Li GX, Xiao Y, Lin S, Lai Y *et al.* Quantitative evaluation of the immunodeficiency of a mouse strain by tumor engraftments. *J Hematol Oncol* 2015; **8**: 59.

39 Duan S, Skaar JR, Kuchay S, Toschi A, Kanarek N, Ben-Neriah Y *et al.* mTOR generates an auto-amplification loop by triggering the betaTrCP- and CK1alpha-dependent degradation of DEPTOR. *Mol Cell* 2011; **44**: 317–324.

40 Gao D, Inuzuka H, Tan MK, Fukushima H, Locasale JW, Liu P *et al.* mTOR drives its own activation via SCF(betaTrCP)-dependent degradation of the mTOR inhibitor DEPTOR. *Mol Cell* 2011; **44**: 290–303.

41 Zhao Y, Xiong X, Sun Y. DEPTOR, an mTOR inhibitor, is a physiological substrate of SCF(betaTrCP) E3 ubiquitin ligase and regulates survival and autophagy. *Mol Cell* 2011; **44**: 304–316.

42 van Stralen E, van de Wetering M, Agnelli L, Neri A, Clevers HC, Bast BJ. Identification of primary MAFB target genes in multiple myeloma. *Exp Hematol* 2009; **37**: 78–86.

43 Mendes RD, Sarmento LM, Cante-Barrett K, Zuurbier L, Buijs-Gladdines JG, Povoa V *et al.* PTEN microdeletions in T-cell acute lymphoblastic leukemia are caused by illegitimate RAG-mediated recombination events. *Blood* 2014; **124**: 567–578.

44 Ren P, Yue M, Xiao D, Xiu R, Gan L, Liu H *et al.* ATF4 and N-Myc coordinate glutamine metabolism in MYCN-amplified neuroblastoma cells through ASCT2 activation. *J Pathol* 2015; **235**: 90–100.

45 Qing G, Yan P, Xiao G. Hsp90 inhibition results in autophagy-mediated proteasome-independent degradation of IkappaB kinase (IKK). *Cell Res* 2006; **16**: 895–901.

46 Hu Y, Su H, Li X, Guo G, Cheng L, Qin R *et al.* The NOTCH ligand JAGGED2 promotes pancreatic cancer metastasis independent of NOTCH signaling activation. *Mol Cancer Ther* 2015; **14**: 289–297.